

# Microearthquake Focal Mechanisms

## A Tool for Monitoring Geothermal Systems

By Bruce R. Julian (U. S. Geological Survey - Menlo Park, CA) and Gillian R. Foulger (University of Durham - Durham, United Kingdom)

Recent studies of complete (moment tensor) source mechanisms show that microearthquakes at geothermal areas often are accompanied by volume changes, which implies that these events involve processes more complicated than simple shear faulting. These volume changes correlate with commercial exploitation activities, with volume decreases restricted largely to exploited fields, indicating that microearthquake mechanisms are potentially useful for monitoring the effects of exploitation upon geothermal systems. The simplest physical explanation of observed mechanisms involves combined shear and tensile failure, but the observed volume changes are smaller than expected for this process, and imply an additional volume-compensating process, probably involving rapid fluid flow. Combined interpretation of source mechanisms and high-resolution hypocenter locations can help to elucidate the processes at work. Practical methods for determining microearthquake moment tensors require networks of ten or more digital three-component seismometers distributed uniformly within about two focal depths of the epicenters. High-quality instrumental monitoring is needed in order to apply modern analysis methods, including high-resolution relative earthquake location and moment-tensor source-mechanism determination, and should have high priority before and during exploitation of geothermal systems.

### Introduction

Traditionally, the term *source mechanism* in seismology has meant *fault-plane solution*, a simplified construct that involves the assumption of pure shear slip on planar faults in isotropic elastic media (e.g. Reasenberg and Oppenheimer, 1985). A fault-plane solution is not a complete theoretical description of a seismic point source, however. Such a description, provided by the *moment tensor* (e.g. Julian and others, 1998), involves two additional source parameters, and in particular allows for volume changes. This greater generality makes possible the description of failure processes that, it is now clear, are common in volcanic and geother-

mal environments (Miller and others, 1998a). The subset of earthquake mechanisms representable by fault-plane solutions consists of *double couples* (DCs), so-called because they are mathematically equivalent to pairs of force couples.

The inappropriate assumption that all geothermal microearthquakes (MEQs) have DC mechanisms obscures the true processes at work, and has prevented seismology from contributing all that it could to geothermal utilization technology. Practical techniques now exist for determining moment-tensor mechanisms of MEQs, and also for locating MEQ hypocenters with high precision. Joint interpretation of source mechanisms and hypocenter distributions can provide valuable information about physical processes in geothermal reservoirs, and far more information than can either type of information by itself.

### Moment-Tensor Determination

Determining complete moment-tensor earthquake mechanisms is considerably more difficult than determining fault-plane solutions. *P*-phase first motion polarities from several seismometers, commonly used to determine fault-plane solutions, almost never can distinguish between DC and non-DC mechanisms, let alone determine full moment tensors accurately (Fig.1). Methods that can do this must extract more information than just first-motion polarities from seismograms, and place greater demands on data quality.

The most widely used methods at present involve fitting theoretical seismograms to waveforms observed on “broad-band” seismometers, whose spectral response must cover at least the frequency band from about 0.1 to 10 Hz in the case of local earthquakes. Waveform-fitting methods work only for events larger than about magnitude 3.5 to 4, so they apply to only the largest geothermal earthquakes (e.g. Dreger and others, 2000).

The amplitudes of seismic waves radiated in different directions from an earthquake depend on the source mechanism, but

Figure 1 - An illustration of the wide range of source mechanisms that typically is compatible with even a high quality set of P-phase polarity observations, after Julian and Foulger (1996). Upper focal hemispheres are shown in equal-area projection. The polarity data shown are for earthquake of 07:41 UTC, Sept. 15, 1991 at the Hengill geothermal area, Iceland, as recorded on a network of portable digital seismometers. Open dots: inward motions; filled dots: outward motions. (a) a DC mechanism that fits the polarity data acceptably, given the reliability of their focal-sphere positions. (b) a more accurate mechanism, with a large isotropic component, derived by inverting body-wave polarities and amplitude ratios simultaneously (Fig. 2).

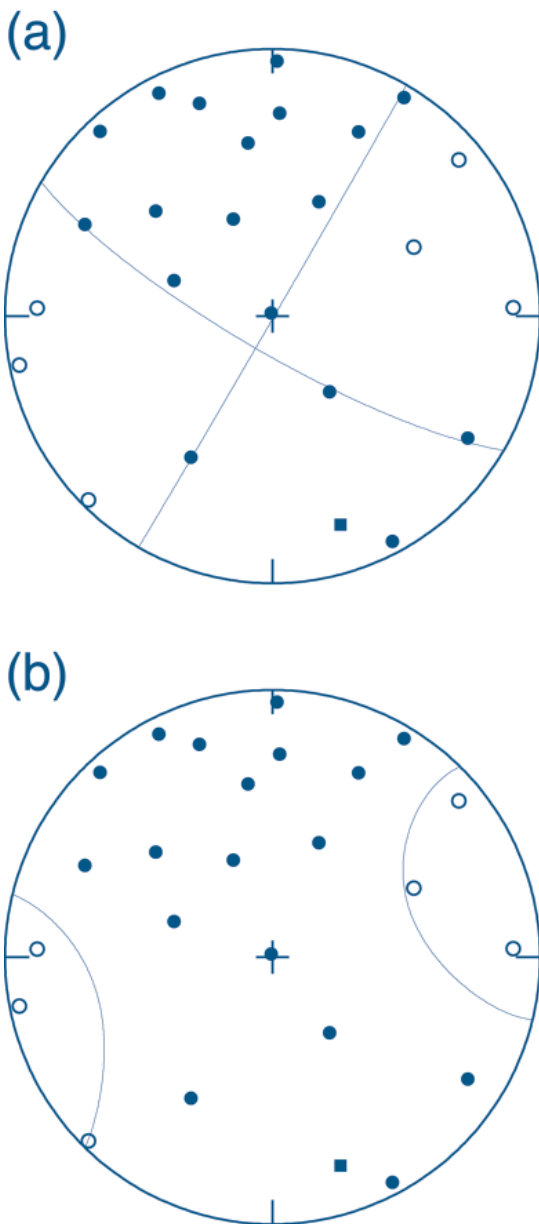
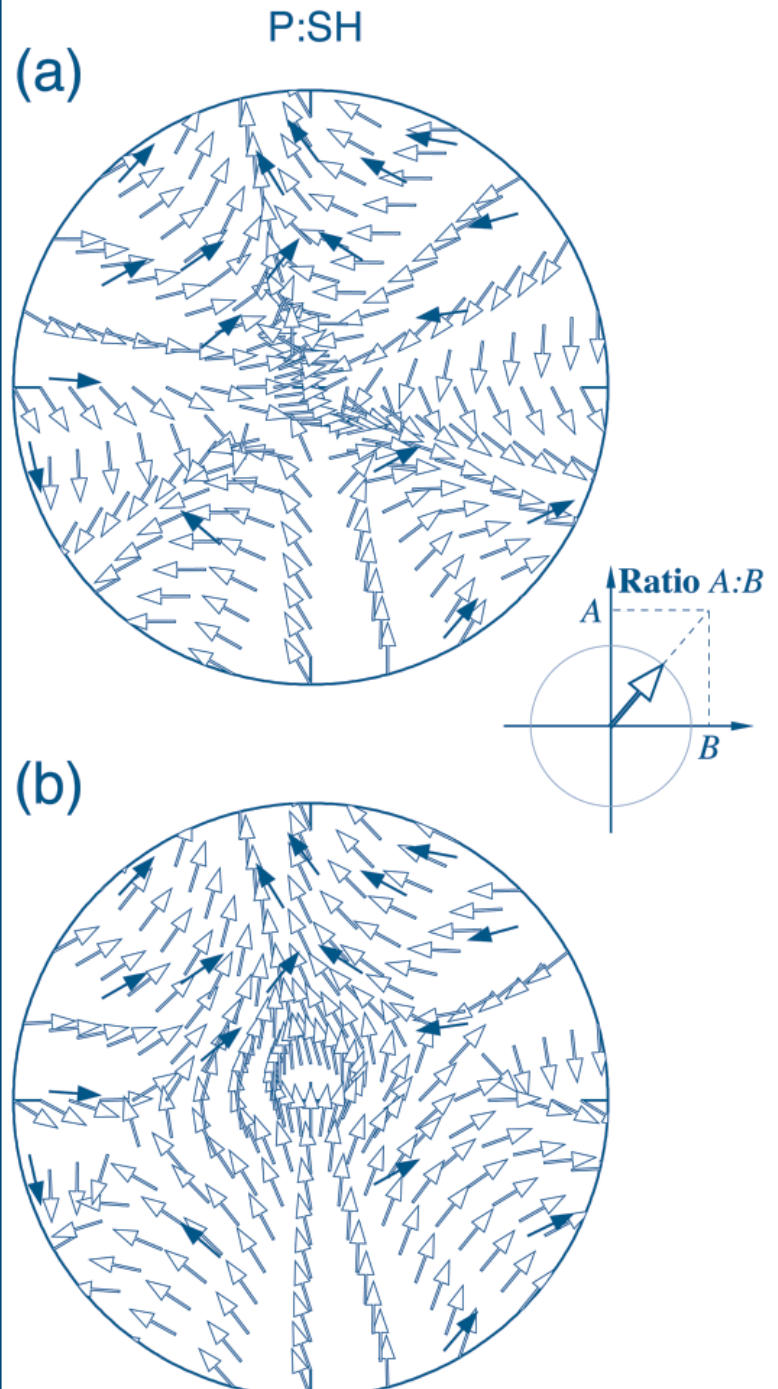


Figure 2 - An example of the use of amplitude ratios to determine focal mechanisms, after Julian and Foulger (1996). The orientation of each small arrow plotted on the upper focal hemisphere represents a P:SH-phase amplitude ratio (see inset), with filled arrows representing observed ratios and open arrows showing theoretical ratios. The (a) DC and (b) non-DC mechanisms correspond to those in Figure 1. The observed amplitude ratios rule out the DC mechanism for this earthquake, but agree well with theoretical ratios for the non-DC mechanism.



observed amplitudes are severely contaminated by wave-propagation effects such as focusing, de-focusing, scattering, and anelastic attenuation, so direct inversion of observed amplitudes to determine source mechanisms works poorly in practice. An effective technique for reducing bias from wave-propagation effects is to invert the ratios of the amplitudes of different seismic phases recorded at a single seismometer (Julian and Foulger, 1996). If phases that have similar propagation paths, such as *P* and *S*, are used, propagation anomalies will be similar, and amplitude ratios will be insensitive to them. Most work to date has used the phases *P* and *SH* (the *S* phase measured horizontally perpendicular to the propagation direction). Theoretical computations indicate that the amplitude ratio for these phases is an order of magnitude less sensitive to shallow near-receiver structure than the raw amplitudes are (Foulger and others, 2004).

An amplitude-ratio analysis of the same earthquake for which Figure 1 shows first-motion polarities is presented in Figure 2. Each

ratio is represented by the direction of a short arrow (Fig. 2 inset), a convention that preserves the signs of both of the amplitudes that enter into the ratio. The agreement between observed (filled arrows) and theoretical (open arrows) ratios is much better for the non-DC mechanism fitted to the amplitude-ratios than they do to the fault-plane solution determined from the *P* phase polarities alone (Fig. 2(a)).

## Studies at Geothermal Areas

In the last decade, investigations using dense networks of digital three-component seismometers and applying the amplitude-ratio method described above have targeted MEQ mechanisms at several geothermal and volcanic areas throughout the world. These include The Geysers in northern California, which is the most heavily exploited geothermal field on Earth (Ross and others, 1999), the Hengill-Grensdalur volcanic complex in southwest Iceland (where the 100-MW (installed) Nesjavellir field had recently be-

**Figure 3 - Focal mechanisms of earthquakes at Long Valley caldera, California. Each circle shows the theoretical far-field *P*-wave polarity pattern on an equal-area projection of the upper focal hemisphere, with the compressional field filled. Red: MEQs from the summer of 1997, when a three-component digital seismometer network operated in the area; blue: *M* 4.5 to 4.9 earthquakes of November 1997, determined from regional broad-band seismograms (Dreger and others, 2000); green: mechanism of the 16:44 event of 25 May 1980, as reported by Julian and Sipkin (1985), which was constrained to be deviatoric.**

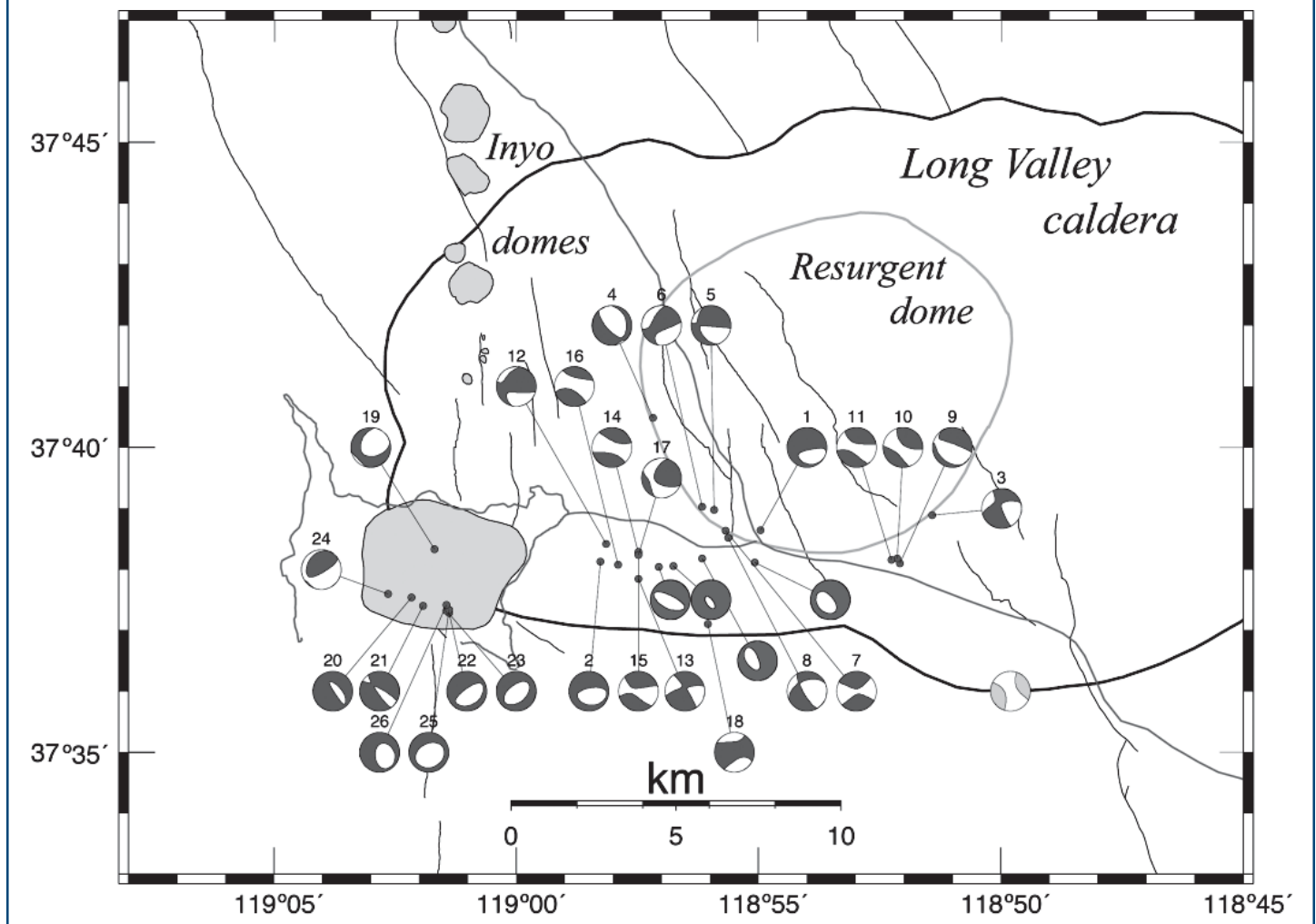
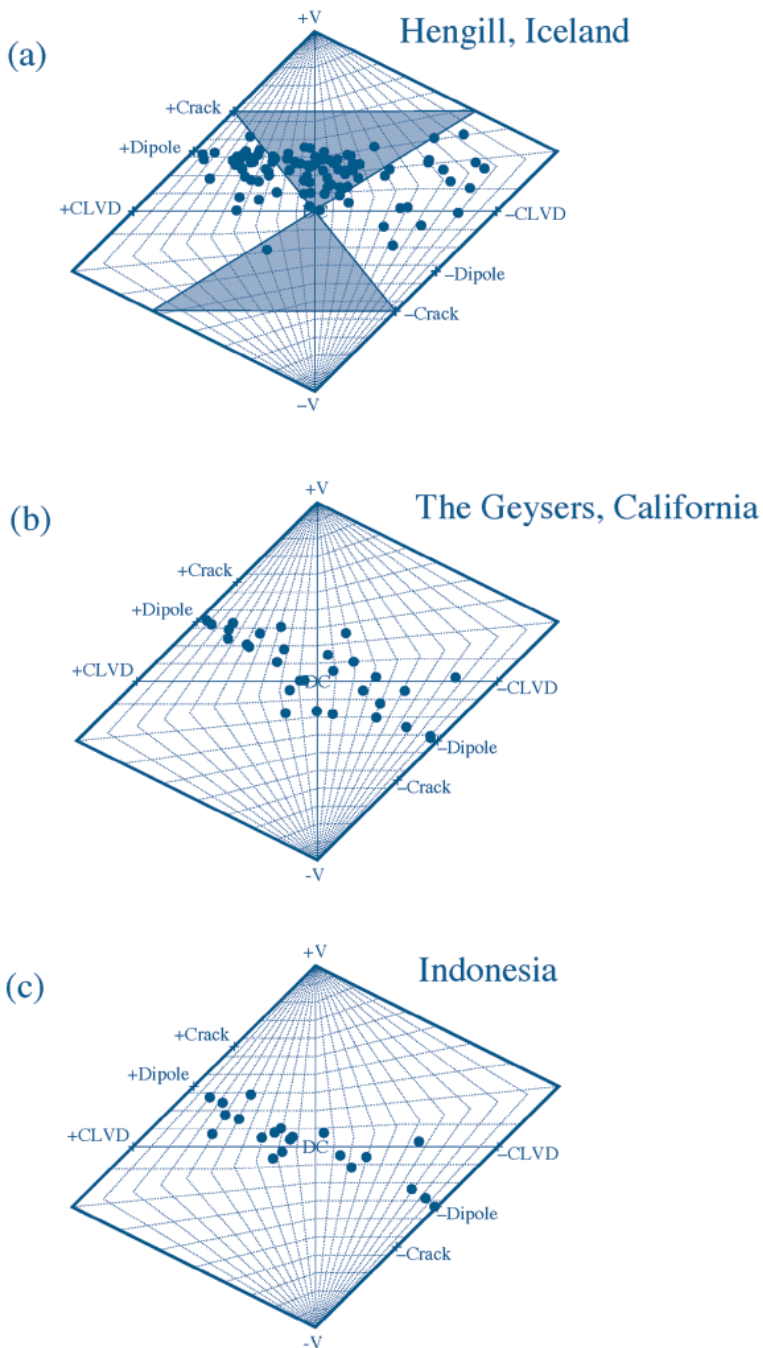


**Figure 4 - Source-type plots of earthquake mechanisms from (a) the Hengill-Grensdalur volcanic complex, Iceland (after Miller and others, 1998b) and (b) The Geysers geothermal area, California (after Ross and others, 1999), and (c) a commercially exploited geothermal area in Indonesia. Mechanisms lying in the top half of the STP involve volume increases, and those in the bottom half involve volume decreases. Mechanisms with no volume change lie on the horizontal line through point DC, the locus of all double couples. Pure isotropic explosions (implosions) lie at the point labeled +V (-V) and opening (closing) tensile cracks lie at point +Crack (-Crack).  $\pm$ Dipole and  $\pm$ CLVD: geometrically defined force systems lacking obvious physical interpretations. The shaded triangles in (a) give the loci of all possible combinations of shear and tensile faulting.**



gun operating) (Miller and others, 1998b), Long Valley caldera, in eastern California (Foulger and others, 2004), and exploited geothermal fields in Indonesia (unpublished results).

Well-determined mechanisms for earthquakes at Long Valley caldera, California, which are broadly similar to the results from the other areas, are shown in Figure 3. Nearly all the mechanisms have similar orientations, consistent with the rapid northeast-southwest extension across the resurgent dome measured geodetically since 1980. Most of the earthquakes have non-DC mechanisms, and most of them indicate volume increases.

### Physical Processes of Non-DC Geothermal Earthquakes

The most likely hypothesis for the physical mechanism of these non-DC earthquakes is that they involve simultaneous shear and tensile faulting, perhaps on separate faults. The observed moment-tensors rule out this simple model, but allow for a slightly more complicated version, which also is physically more likely to occur in the Earth.

*Source-type plots* (Hudson and others, 1989) are shown in Figure 4 for microearthquakes at three geothermal areas, two of which (The Geysers and an Indonesian field) are heavily exploited. This type of display shows earthquake mechanisms in a manner independent of the source orientation (that is, position on the plot depends only on the ratio of the principal moments). All combinations of shear and tensile faulting, with whatever orientations and relative strengths, lie within the shaded triangles shown in Figure 4(a), with the upper triangle corresponding to cases with opening tensile fractures. Mechanisms with the most plausible relative orientations of the fractures lie just inside the triangles, near the line between the +Crack and -Crack points.

The observed source types are not in accord with this expectation, however. Only at the Hengill-Grensdalur complex do significant numbers of mechanisms fall within the triangle. At The Geysers, the Indonesian field, and Long Valley caldera (not shown), most mechanisms lie outside the triangles, in positions corresponding to smaller volume changes. Thus, if these earthquakes involve combined shear and tensile fractures, they must also involve some additional process that reduces the magnitude of the volume change, such as a pressure drop in the fluid filling the tensile crack, and/or the rapid migration of fluid into the crack.

Earthquake source types also correlate strongly with exploitation of geothermal fields. At the lightly exploited Long Valley caldera and Hengill-Grensdalur complex, most of the earthquakes have volume increases. At the two significantly exploited areas though, The Geysers and the Indonesian field, volume decreases and increases

are about equally numerous. The common occurrence of volume decreases probably indicates the collapse of pre-existing cavities in response to decreases in pore pressure.

## High-Resolution Hypocenter Locations

Even though full moment-tensor earthquake mechanisms contain much more information than fault-plane solutions, this information still is not adequate to uniquely diagnose the physical processes at work. Different physical processes can have identical equivalent force systems, and they will radiate identical seismic waves and have identical source mechanisms. To diagnose physical processes, other types of data must be used.

One of the most promising approaches is to use the locations of MEQ hypocenters to delimit the geometry of the failure zone. For example, because shear fractures are oriented at angles of  $45^\circ$  to the  $P$  and  $T$  principal axes of the focal mechanism and tensile fractures are normal (at  $90^\circ$ ) to the  $T$  axes, it is possible to distinguish these types of fractures by comparing source-mechanism orientations with fracture orientations revealed by hypocenter locations. This approach has only recently become practical, because of the development of new hypocenter-determination techniques, such as that of Waldhauser and Ellsworth (2000), that are far more precise than previous methods (Fig. 5).

The earthquakes at Long Valley caldera shown in Figures 3, 5 and 6 provide a good example. High-resolution hypocenters of an earthquake cluster that includes events 9, 10, and 11 clearly delineate a vertical WNW-striking failure surface (Figs. 5b, 6), which is not evident from hypocenters in standard catalogs (Fig. 5a). This fault plane has precisely the orientation expected for a tensile fracture consistent with the focal mechanisms for these three earthquakes (Foulger and others, 2004), and strongly supports the hypothesis that tensile fracturing plays a major role in the source processes of these non-DC earthquakes. Combining moment-tensor determination with high-resolution hypocenter location shows great promise for clarifying the source physics of geothermal earthquakes and understanding the distribution of fluid properties and flow in exploited reservoirs.

The high-resolution hypocenters in Figures 5 and 6 are derived from arrival-time measurements made from individual seismograms. An alternative technique, cross-correlation of signals from nearby seismometers, can give much more accurate relative locations than even those shown here. These ultra-high-precision methods require high-quality digital seismograms, though, so current practices such as using analog telemetry and digital recording should be abandoned for microearthquake analyses in geothermal systems.

## Summary

Applying new seismological techniques to microearthquakes in geothermal systems can provide knowledge of the physical state and processes of potential value both for geothermal prospecting and for monitoring fields during energy production. Older methods, such as single-event hypocenter location techniques and derivation of fault-plane solutions rather than full (moment-tensor) source mechanisms, are inaccurate and based on assumptions that are incorrect in geothermal areas. These new techniques require high-quality three-component digital seismic data, and acquisition of this data, both before and during geothermal exploitation, should have high priority. ■

**Figure 5 - Comparison of conventional and high-resolution earthquake locations. Top: Map of south moat and southern resurgent dome of Long Valley caldera, showing epicenters of earthquakes from May 25 to Sept. 12, 1997, taken from the Northern California Seismograph Network (NCSN) catalog. Bottom: Same, showing earthquake epicenters computed using the high-resolution algorithm of Waldhauser and Ellsworth (2000). The high-resolution results show extensive small-scale structure not evident in the catalog hypocenters. A more detailed view of the earthquakes within the oblique rectangle is shown in Figure 6.**

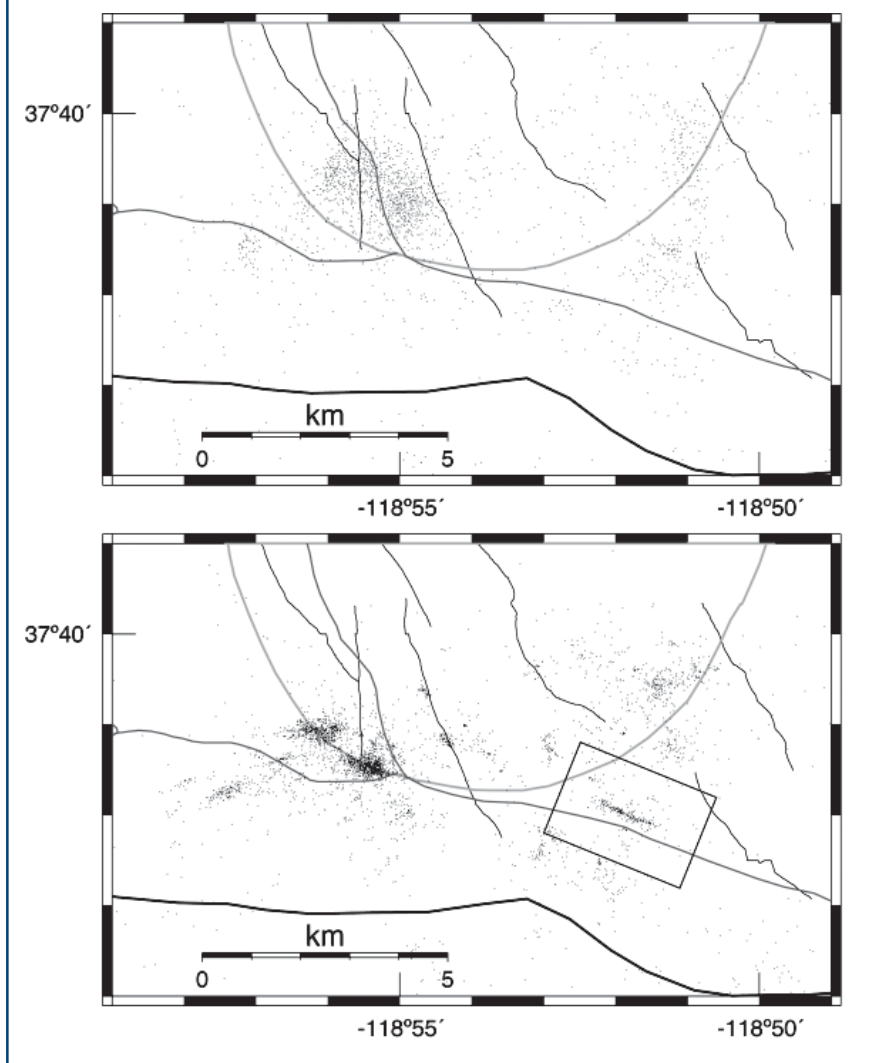
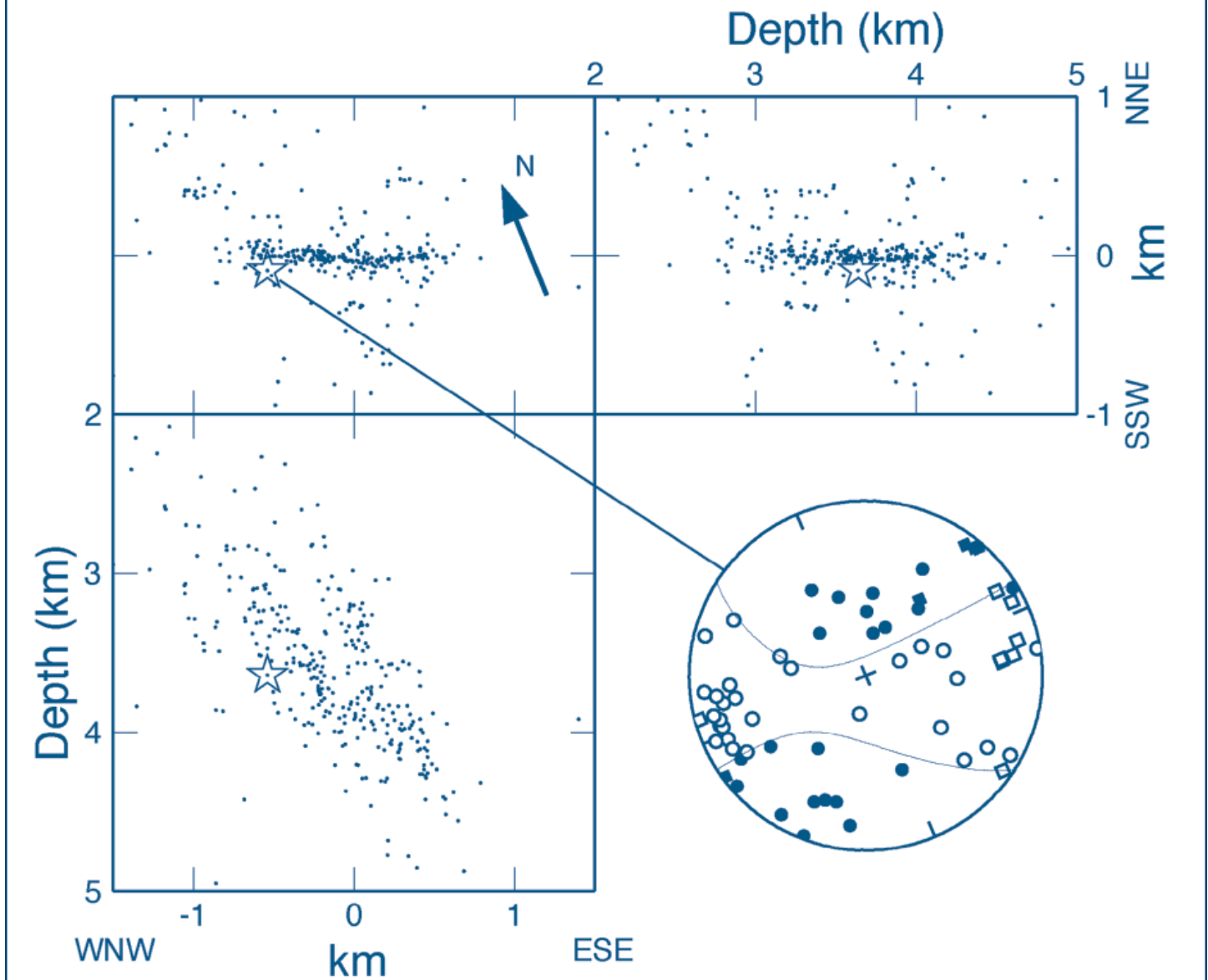


Figure 6 - Tensile fracture identified by comparing microearthquake focal mechanisms and high-resolution hypocenters, after (Foulger and others, 2004). Views from three orthogonal directions showing the locations of the 314 earthquakes (black dots) within the oblique rectangle of Figure 5 that lie between 2 and 5 km depth. Upper left: map view; upper right: SSW-NNE vertical cross-section (viewing direction: 292°); lower left: WNW-ESE vertical cross-section (viewing direction: 22°). Star: earthquake 11 (see Fig. 3). Lower right: Mechanism of earthquake 11, shown as an upper-hemisphere plot of P-phase polarities, and nodal curves of the derived focal mechanism. The focal sphere is rotated in the same manner as the map at upper left, so that the fault plane defined by the seismicity is horizontal in the figure. The mechanism for this earthquake is compatible with tensile fracturing on this plane, but not with shear fracturing.



## References

- Dreger, D.S., H. Tkalčić, and M. Johnston, M., 2000. "Dilational Processes Accompanying Earthquakes in The Long Valley Caldera." *Science*, v. 288, no. 5463, pp. 122-125.
- Foulger, G.R., B.R. Julian, D.P. Hill, A.M. Pitt, P.E. Malin, and E. Shalev, 2004. "Evidence of Hydraulic Fracturing in Non-Double-Couple Microearthquakes at Long Valley Caldera, California." *Journal of Volcanology and Geothermal Research*, v. 132, no. 1, pp. 45-71.
- Hudson, J.A., R.G. Pearce, and R.M. Rogers, 1989. "Source Type Plot for Inversion of the Moment Tensor." *Journal of Geophysical Research*, v. 94, no. B1, pp. 765-774.
- Julian, B.R., and G.R. Foulger, 1996. "Earthquake Mechanisms from Linear-Programming Inversion of Seismic-Wave Amplitude Ratios: *Bulletin of the Seismological Society of America*, v. 86, no. 4, pp. 972-980.
- Julian, B.R., A.D. Miller, and G.R. Foulger, 1998. "Non-Double-Couple Earthquakes I. Theory." *Reviews of Geophysics*, v. 36, no. 4, pp. 525-549.
- Julian, B.R., and S.A. Sipkin, 1985. Earthquake Processes in The Long Valley Caldera Area, California. *Journal of Geophysical Research*, v. 90, no. B13, pp. 11155-11169.
- Miller, A.D., G.R. Foulger, and B.R. Julian, 1998a. "Non-Double-Couple Earthquakes II. Observations." *Reviews of Geophysics*, v. 36, no. 4, pp. 551-568.
- Miller, A.D., B.R. Julian, and G.R. Foulger, G.R., 1998b. "Three-Dimensional Seismic Structure and Moment Tensors of Non-Double-Couple Earthquakes at the Hengill-Greisdalur Volcanic Complex, Iceland." *Geophysics Journal International*, v. 133, no. 2, pp. 309-325.
- Reasenber, P., and D. Oppenheimer, 1985. *FPPFIT, FPPLLOT and FPPAGE: Fortran Computer Programs for Calculating and Displaying Earthquake Fault-Plane Solutions*. USGS Open File Report 85-739.
- Ross, A., G.R. Foulger, and B.R. Julian, 1999. "Source Processes of Industrially Induced Earthquakes at The Geysers Geothermal Area, California." *Geophysics*, v. 64, no. 6, pp. 1877-1889.
- Waldhauser, F., and W.L. Ellsworth, 2000. "A Double-Difference Earthquake Location Algorithm: Method and Application to the Northern Hayward Fault, California." *Bulletin of the Seismological Society of America*, v. 90, no. 6, p. 1353-1368.